



Non-destructive carrier concentration determination in InAs thin films for THz radiation generating devices using fast differential reflectance spectroscopy

Michał A. Kozub¹ · Marcin Motyka¹ · Mateusz Dyksik¹ ·
Grzegorz Sęk¹ · Jan Misiewicz¹ · Kazuichi Nishisaka² ·
Toshihiko Maemoto² · Shigehiko Sasa²

Received: 11 March 2016 / Accepted: 9 July 2016 / Published online: 18 July 2016
© The Author(s) 2016. This article is published with open access at Springerlink.com

Abstract We present a fast and robust optical method of determining carrier concentrations in heavily doped layered structures. We discuss several advantages of the technique as compared to other, more commonly applied methods using as an example InAs based devices used for THz radiation generation. Our approach leads to a more accurate estimation of doping levels in the investigated structures and aids the standard Hall measurements in precise predictions of radiative efficacy in the THz region. Predicted enhancement factors reproduce THz-Time Domain Spectroscopy (TDS) experiment results within a 2 % accuracy.

Keywords FDR · Doping density · Carrier concentration · THz · InAs

1 Introduction

The knowledge of doping levels in semiconductor structures may be considered paramount from the point of view of fabrication of many devices requiring either n- or p-type doped layers. This is the case for both lasers and detectors based on p-n junctions. The same is

This article is part of the Topical Collection on TERA-MIR: Materials, Generation, Detection and Applications.

Guest Edited by Mauro F. Pereira, Anna Wojcik-Jedlinska, Renata Butkute, Trevor Benson, Marian Marciniak and Filip Todorov.

✉ Michał A. Kozub
michal.kozub@pwr.edu.pl

¹ Laboratory for Optical Spectroscopy of Nanostructures, Department of Experimental Physics, Faculty of Fundamental Problems of Technology, Wrocław University of Science and Technology, Wybrzeże Wyspiańskiego 27, 50-229 Wrocław, Poland

² Nanomaterials Microdevices Research Center, Osaka Institute of Technology, 5-16-1 Omiya, Asahi-ku, Osaka 535-8585, Japan

true for photonic devices where obtainable improvement is largely dependent on doped layers owing to the plasmon enhancement effect (N'Tsame Guilengui et al. 2012). Finally, it is an extremely significant factor in the case of terahertz emitters utilizing InAs doped layers (Kozub et al. 2015) and also in case of mid infrared semiconductor lasers (both Quantum Cascade Lasers (QCLs) Ohtani and Ohno 2003; Teissier et al. 2004 as well as Interband Cascade Lasers (ICLs) Yang 1995), where doped InAs layers are used for a plasmon-based enhancement of waveguiding properties (Tian et al. 2010). The method of our choice for the determination of carrier concentrations is the Fast Differential Reflectivity (FDR) method (Motyka and Misiewicz 2010). In the paragraphs to follow we discuss it's advantages above other commonly used techniques. In this work we focus on InAs based THz emitters utilizing the Photo-Dember effect for radiation generation (Kozub et al. 2015). They can be classified among semiconductor surface generation methods which constitute one branch of THz sources beside the commonly used low temperature (LT) grown GaAs antennas and organic crystals (4-N,N-dimethylamino-4'-N'-methyl stilbazolium tosylate (DAST) crystals being perhaps the most notable). One significant advantage of these generation methods is the ease of pump beam alignment when compared to LT-GaAs antennas and lower average pump beam power then usually present in organic crystals. This makes InAs emitters enticing for various THz applications, however to efficiently characterize them one needs to know the level of carrier concentration within one of it's layers.

2 Sample and experiment description

For the aforementioned application we fabricated a series of samples consisting of InAs grown on SI-GaAs in a Anelva molecular beam epitaxy (MBE) reactor. We can distinguish two layers of InAs in our structures: the top one—serving as an active layer—where generation of THz frequency radiation occurs; and a bottom one—directly adjacent to GaAs—that serves as a reflection layer and is highly doped. Additionally, doping of the bottom (reflection) layer was done with two distinct doping techniques: uniform- and δ (delta)-doping (the efficacy of this generation method, including experimental details, has been discussed elsewhere Kozub et al. 2015). Silicon was used as the doping agent in order to achieve high, n-type, conductivity of InAs—the proper Si cell temperature, corresponding to any particular requested carrier concentration (what is referred to later in text as 'nominal' or 'intended'), was determined by a calibration curve from a doped InAs test structure. Multiple samples have been investigated: the first two, where the nominal concentration was $5 \times 10^{18} \text{ cm}^{-3}$ (samples 1 and 2); another, where it was $5 \times 10^{19} \text{ cm}^{-3}$ (sample 3); and finally, sample 4, where δ -doping was utilized, with an intended density of $1 \times 10^{20} \text{ cm}^{-3}$ – sample critical parameters have been summed up in Table 1.

Table 1 Investigated sample characteristics, where w_A is the active layer, w_R - reflection layer, n - nominal carrier concentration

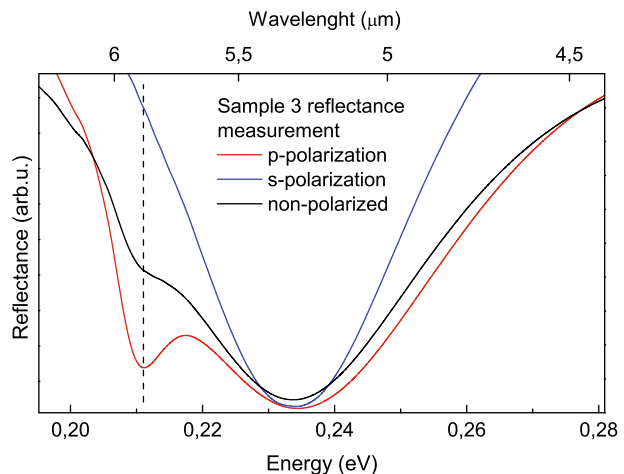
Sample	w_A (nm)	w_R (nm)	n (cm^{-3})
1	1000	500	5×10^{18}
2	1000	500	5×10^{18}
3	1000	500	5×10^{19}
4	1200	200	1×10^{20}

Since post growth characterization can be an issue in a strictly manufacturing environment, usually due to limited experimental options, there is a strong need for optimization of employed measurement facilities. At present there is a limited number of experiments allowing for the acquisition of information regarding carrier concentration in semiconductor layers or low dimensional semiconductor structures. We can distinguish electrical methods like Hall measurements or capacity-voltage (CV) measurements—unfortunately they all require special sample preparation, i.e. proper contact fabrication and also, as is the case in Hall measurements, the additional application of an external magnetic field. In contrast to electrical approaches, the existence of contactless methods should also be noted. Optical spectroscopy experiments utilizing e.g. reflectance (Hinkey et al. 2011; Berreman 1966), transmittance (Ye et al. 2013) and ellipsometry (Raman et al. 2011) measurements should be mentioned here and can be broadly classified as such.

We use a modified reflectance approach at the origin of which lies the phenomenon first described by Berreman (1966) in the context of dielectric films deposited on metals. Due to the enhancement of the normal electric field component of incident light, that occurs when the permittivity $\epsilon(\omega)$ approaches 0 at the plasmon frequency, we can observe a characteristic change in the absorption spectrum. At the microscopic level these changes were ascribed to losses Γ of the phonons. However, in the context of metals, absorption is due to the free carriers of the surface plasmon polariton mode, in turn named the 'Brewster' mode (Vassant et al. 2012)—which is more appropriate in our case. We present this effect in a reflectance measurement in Fig. 1. Since there is a need for the electric field of the incoming light to have non-zero components in the sample growth direction, therefore measurements at oblique angles are preferable—in our case at a 45° angle.

Our experimental setup is based on a Bruker Vertex 80 spectrometer. The measurements have been performed utilizing a rather complex experimental configuration (Motyka et al. 2009a), as it has also many other functionalities, but in principle the same results should be possible to obtain by using the simplest Fourier spectrometer and a modulating laser. The laser itself is a CW, single mode semiconductor laser giving 40 mW of average power at the 661nm wavelength with a spot size of 1mm^2 . Such conditions yield $\sim 10^{15}\text{cm}^{-3}$ photogenerated carriers, a value greatly below our measured densities, thus having no effect on obtained results. In the FDR approach (Motyka and Misiewicz 2010;

Fig. 1 Experimental manifestation of the Brewster mode as observed in a reflection measurement. The typical absorption dip disappears only in the case of one particular polarisation of incident radiation, whereas it should be visible in others



Motyka et al. 2011) a rapid scan experiment mode greatly limits the acquisition time of experimental data—typically to the order of single minutes—which is of high importance, especially when similar methodology is used on an industrial level.

The wavenumber position of the p-polarisation dip is obtained through a third derivative Lorentzian fit of the spectra. As we have shown in our previous work (Motyka et al. 2009b), such a fit can give us a spectral resolution better than 10 meV—which means that even in the worst case scenario, of overlapping spectral features, we can separate two carrier concentration signals differing by about $1 \times 10^{18} \text{cm}^{-3}$. In the case, however, of a single doped layer—which is what we are dealing with—the source of the signal is easy to pin-point and a more accurate estimation of the peak position is possible.

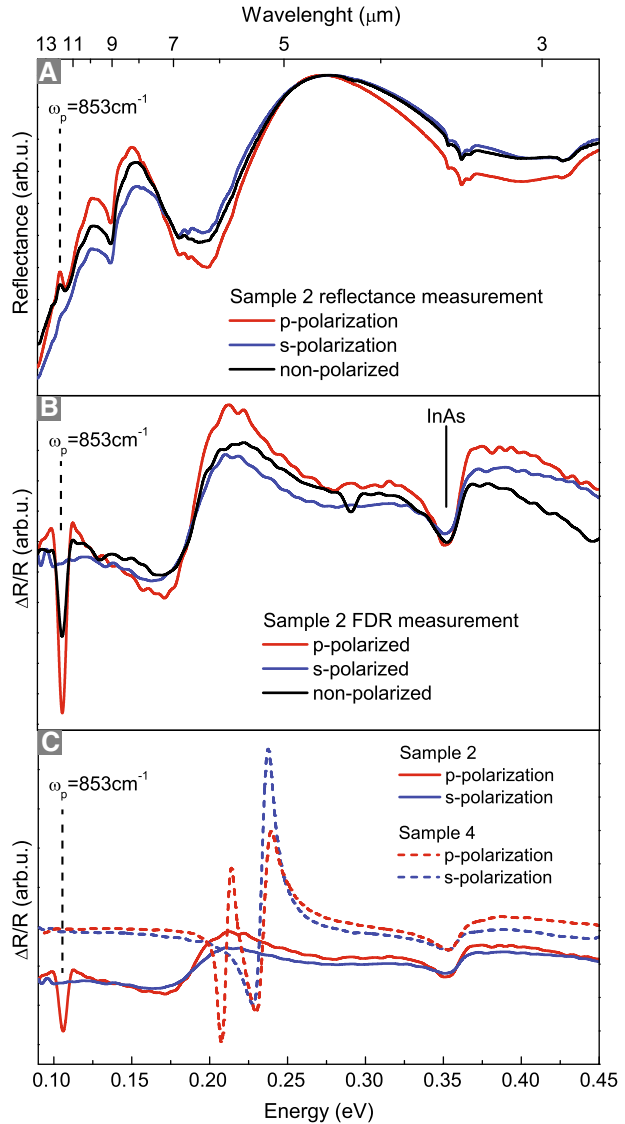
3 Results and discussion

Figure 2 shows a comparison of obtained results between a standard reflectivity measurement (panel A) and the FDR (panel B) method for the same sample. The standard reflectivity measurement displays a plethora of spectral features, however, important information might end obfuscated or even unextractable to the untrained eye. Therefore the most notable difference between those two are the very well pronounced optical transitions in the FDR method signifying the base transition of InAs at 0.35 eV and the plasma edge at around 0.11 eV. As we should only expect these two features in the measured spectra, it is possible to extract carrier densities without the need for polarizers, further simplifying the experiment. Panel C of Fig. 2 shows FDR spectra of a single sample of each set exhibiting the greatest span in wavenumbers corresponding to their plasma edge. Each sample shows the plasma edge absorption in a different spot on the wavenumber (and energy) scale corresponding to the samples factual carrier density.

Given the results of FDR measurements we can determine carrier concentrations based on the plasma resonance position by cross-referance comparison with the experiment of Hinkey et al. (2011). Therein the authors show a clear dependancy between carrier concentration and the plasma edge absorption feature position based on reflectance measurements. Their findings (black squares), together with a power law fit of experimental data, have been shown in panel A of Fig. 3. By using the aforementioned fit function, we can project the positions of the plasma edge absorption of our samples, gathered through FDR measurements, onto the extracted dependancy and thereby obtain their corresponding carrier concentration. The result of such a comparison has been depicted in panel B of Fig. 3. We can clearly see a high divergence between intended and actual concentration values in the higher carrier density region.

Given the knowledge we aquired through FDR measurements and compared with Hall in Table 2—we can see greater discrepancy between the two in the higher density region. For a Hall measurement in the van der Pauw configuration, uncertainty is usually ascribed to imperfections of geometry of the system under investigation, i.e. the finite contact length along and perpendicular to sample edges but also a non-zero distance of the contact from the periphery. Taking this into account it is common to expect accuracy better than 5 % when given enough care to sample preparation. However, noise can often exceed this level, especially for low carrier concentration samples or low mobility ones—the latter may be the case for our samples with the highest carrier concentrations, where mobility is

Fig. 2 Panel **a** Reflectance measurement of sample 2 with a barely showing absorption feature at 853 cm^{-1} . Panel **b** The same sample in an FDR experiment—plasma absorption becomes well pronounced and distinguishable, the same is true for InAs base transition. Panel **c** FDR results for two samples exhibiting extreme plasma edge positions and therefore extreme carrier concentrations. InAs base transitions have been included to show the static nature of this feature despite changing dopant densities



the lowest. We may now move on to quantify the efficiency of THz radiation generation of our samples. There is a manifold of approaches that may give us insight into the improvement introduced by the incorporation of a reflection layer, and, thanks to the results of Hall measurements, i.e. the fact that we have access to mobility/density pair values for each of the sample, we may calculate the enhancement factor, defined as the ratio between peak electric field amplitude of our samples' emission to the peak electric field amplitude of a bulk InAs crystal under same excitation conditions. This value can be expressed as a function of reflectivity of the air/active layer interface and active/reflection layer interface:

Fig. 3 Panel A Optical determination of carrier concentration obtained via reflectance measurements by Hinkey et al. (2011). Panel B Projection of our experimental data onto the power law fit seen in panel A. Hall carrier concentration values have also been projected onto this dependency to show their expected wavenumber values

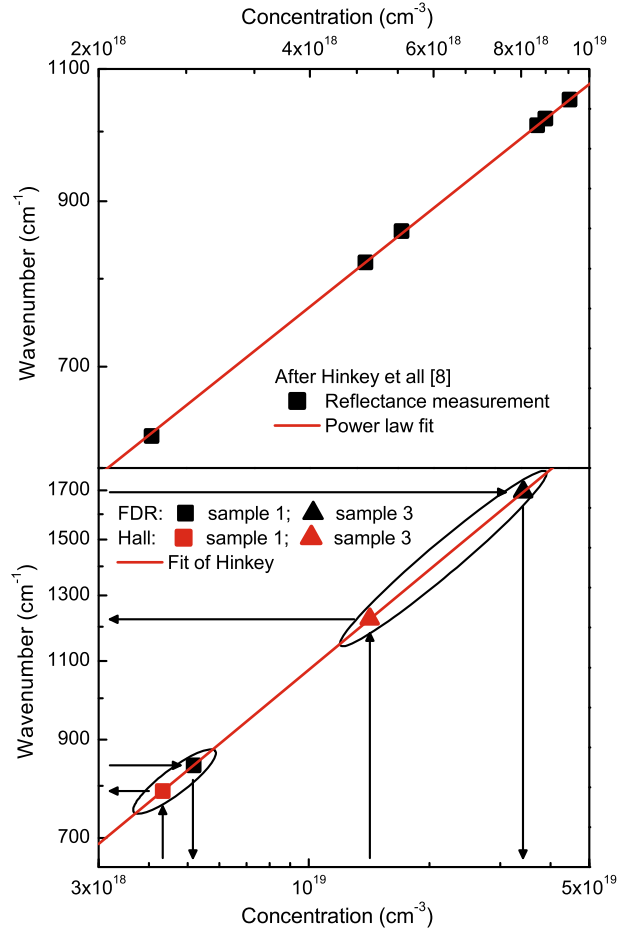


Table 2 Summary of carrier concentrations in the investigated structures and a comparison between experimental methods

Sample	Carrier concentration (cm ⁻³)		
	Intended	FDR	Hall
1	5 × 10 ¹⁸	5.18 × 10 ¹⁸	4.33 × 10 ¹⁸
2	5 × 10 ¹⁸	5.34 × 10 ¹⁸	6.64 × 10 ¹⁸
3	1 × 10 ¹⁹	3.43 × 10 ¹⁹	1.44 × 10 ¹⁹
4	1 × 10 ^{20*}	3.26 × 10 ¹⁹	7.8 × 10 ¹⁹

In the case of sample 4 (marked with *) delta doping was used and the number given would be the equivalent carrier concentration for uniform doping

$$F = \frac{I_t}{I_b} = \frac{1 + R_b}{1 - R_b R_t}, \tag{1}$$

where I_t is the THz emission intensity from a thin film of InAs, I_b is the intensity of emission from bulk InAs and $R_{b,t}$ are the reflectivities of the bottom and top interfaces respectively. This formula, used previously in Kozub et al. (2015), allows for a rough estimation of reflectivity in the Drude model taking mobility/density pairs as input, and returning the expected enhancement factor as a result, which was in fair agreement with THz-TDS measurements.

To make predictions about the expected enhancement factor in our samples we use carrier concentration numbers obtained through the FDR experiment combined with mobility values stemming from Hall measurements. Since in the Hall experiment both the mentioned values are laden with some uncertainty, therefore a more accurate determination of one of them should be reflected in a more realistic prediction of the enhancement factor.

The divergance between FDR- and Hall-originating reflectivity values has been depicted in Fig. 4, for samples 1 to 4—the circles correspond to FDR measured carrier concentrations and it's corresponding reflectivity and squares denote results obtained by Hall measurements. Two of the samples should exhibit similar values of enhancement as they lie nearly on the same isopleth—these do not add to our understanding. On the other hand, for the last two samples there should be a significant difference observable. For sample #4 these points represent a reflectivity shift from 0.774 to 0.673 that further leads to THz enhancement factors of 2.15 instead of the expected 2.38 when one would only be using Hall measurements. Similarly, for sample #3, the expected reflectivity will get upgraded from 0.49 to 0.63 leading to an enhancement factor rise -1.78 up to 2.07. This is summarized in Table 3, where we compare the expected (calculated) enhancement factors with ones obtained through THz-TDS. In this table we also included a comparison of values obtained by the adherence to the approach of Talierco et al. (2014) as opposed to the ones from Hinkley et al. (2011). The difference between the two being the dependency of wavenumber position of the plasma edge on carrier density—for Talierco it shifts slightly towards higher densities at any given wavenumber which ultimately leads us to

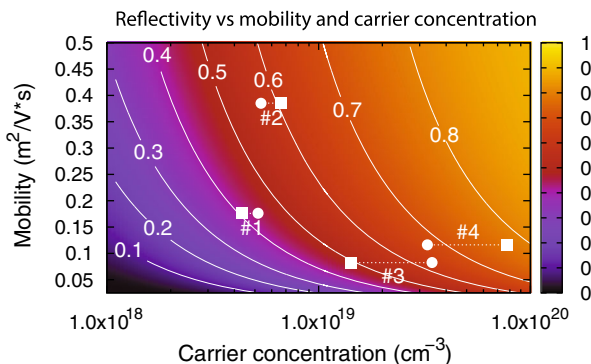


Fig. 4 Reflectivity between the top InAs active layer and the reflection layer calculated in the Drude model. The reflectivity is calculated for a frequency of 1 THz given the following assumptions: mobility of top InAs layer is $4000 \text{ cm}^2/\text{V} \cdot \text{s}$ and its carrier density $1 \times 10^{15} \text{ cm}^{-3}$. The *shapes* show results obtained for our samples, the *squares* and *circles* represent Hall- and FDR-originating carrier concentrations; mobility values in both cases have been taken from Hall experiment

Table 3 Enhancement factors for investigated samples based on: F_M —direct determination via THz-TDS experiment; F_H —Hall measurements; F_{R_1} —FDR approach based on Hinkey et al. (2011); F_{R_2} —FDR approach based on Talierco et al. (2014); Δ_H —relative divergence of Hall-experiment based enhancement factor from measured one; Δ_{R_i} —relative divergence of FDR-originating enhancement factor from experimental value for two approaches: Hinkey’s and Talierco’s

Sample	F_M	F_H	F_{R_1}	F_{R_2}
3	2.15	1.78	2.07	2.11
4	2.22	2.38	2.15	2.20
Sample	F_M	$\Delta_H(\%)$	$\Delta_{R_1}(\%)$	$\Delta_{R_2}(\%)$
3	2.15	17	3.9	1.7
4	2.22	7.3	3.1	1.0

greater enhancement factor values. This divergence is the result of a slightly different take on the effective mass modification due to the non-parabolicity of the conduction band in both papers. The approach of Hinkey et al. was slightly more theoretical and used the $8k \cdot p$ model at its basis, where the non-parabolicity coefficient α is related to the degree of admixture of s-like conduction band states and p-like valence band states. Taliercos’ approach on the other hand obtained its λ_p on N relationship empirically, i.e. by a power law fit of InAs data from ref. Mikhailova (1996). It should be noted, however, that we in no way try to adjudicate about the validity of one approach above the other—since the THz-TDS experiment, that we are using as the basis of comparison, is in itself laden with some uncertainty.

Thanks to Fig. 4 we can understand the discrepancy between the expected radiation enhancement factor (from Hall) and actual enhancement (Table 3) at higher carrier concentrations due to differences in reflectivity—reflectivity values can be either under- or overestimated because of the high uncertainty of the measured carrier concentration obtained through Hall measurements, especially in the higher density region. Fortunately, in either case, with FDR one can get a more realistic estimation of carrier densities and thus, of the radiation enhancement itself—an enhancement that can only be ascribed to the presence of a highly doped reflection layer.

4 Summary

In this work we determined the carrier concentrations of a set of samples intended for THz generating devices by using the Fast Differential Reflectivity method. This allowed us to more accurately predict the generated THz field intensity as compared to a standard Hall measurement—from an 17 % discrepancy to one of around 2 %—and above that, our procedure did not require any post processing of the samples. We compared the aforementioned technique with a standard reflectivity measurement to highlight the advantages of our approach, i.e. ease of analysis, impunity to background noise and material features as well as set-up characteristics. Therefore we argue that the FDR method should become the go-to method for quickly (on the order of single minutes per sample) determining carrier concentrations in layered semiconductor structures.

Acknowledgments This work was partly realized within Grant of National Science Center No. DEC-2011/03/D/ST3/02640.

Open Access This article is distributed under the terms of the Creative Commons Attribution 4.0 International License (<http://creativecommons.org/licenses/by/4.0/>), which permits unrestricted use, distribution, and reproduction in any medium, provided you give appropriate credit to the original author(s) and the source, provide a link to the Creative Commons license, and indicate if changes were made.

References

- Berreman, D.W.: Infrared absorption at longitudinal optic frequency in cubic crystal films. *Phys. Rev.* **130**, 2193–2198 (1966)
- Hinke, R.T., Tian, Z., Yang, R.Q., Mishima, T.D., Santos, M.B.: Reflectance spectrum of plasmon waveguide interband cascade lasers and observation of the Berreman effect. *J. Appl. Phys.* **110**, 043113 (2011)
- Kozub, M., Nishisaka, K., Maemoto, T., Sasa, S., Takayama, K., Tonouchi, M.: Reflection layer mediated enhancement of terahertz radiation utilizing heavily-doped InAs thin films. *J. Infrared Millim. Terahertz Waves* **36**(3), 423–429 (2015)
- Mikhailova, M.P.: Indium arsenide (InAs). In: Levinshtein, M., Rumyantsev, S., Shur, M. (eds.) *Handbook series on semiconductor parameters*, vol. I, pp. 147–168. World Scientific, Singapore (1996)
- Motyka, M., Sęk, G., Misiewicz, J., Bauer, A., Dallner, M., Hoeffling, S., Forchel, A.: Fourier transform photoreflectance and photoluminescence of mid infrared GaSb-based type II quantum wells. *Appl. Phys. Express* **2**, 126505 (2009a)
- Motyka, M., Gelczuk, L., Dąbrowska-Szata, M., Serafinczuk, J., Kudrawiec, R., Misiewicz, J.: Photoreflectance study of partially relaxed epitaxial InGaAs on GaAs. *Opt. Appl.* **39**(3), 561–570 (2009b)
- Motyka, M., Sęk, G., Janiak, F., Misiewicz, J., Kłos, K., Piotrowski, J.: Fourier-transformed photoreflectance and fast differential reflectance of HgCdTe layers. The issues of spectral resolution and Fabry–Perot oscillations. *Meas. Sci. Technol.* **22**, 125601 (2011)
- Motyka, M., Misiewicz, J.: Fast differential reflectance spectroscopy of semiconductor structures for infrared applications by using fourier transform spectrometer. *Appl. Phys. Express* **3**, 112401 (2010)
- N’Tsame Guilengui, V., Cerutti, L., Rodriguez, J.B., Tournié, E., Taliercio, T.: Localized surface plasmon resonances in highly doped semiconductors nanostructures. *Appl. Phys. Lett.* **101**(16), 161113 (2012)
- Ohtani, K., Ohno, H.: InAs/AlSb quantum cascade lasers operating at 10 μm . *Appl. Phys. Lett.* **82**(7), 1003–1005 (2003)
- Raman, R., Mishra, P., Kapoor, A.K., Muralidharan, R.: Origin of Berreman effect in GaN layers on sapphire substrates. *J. Appl. Phys.* **110**(5), 0–5 (2011)
- Taliercio, T., Guilengui, V.N., Cerutti, L., Tournié, E., Greffet, J.J.: Brewster “mode” in highly doped semiconductor layers: an all-optical technique to monitor doping concentration. *Opt. Express* **22**(20), 24294–24303 (2014)
- Teissier, R., Barate, D., Vicet, A., Alibert, C., Baranov, A.N., Marcadet, X., Renard, C., Garcia, M., Sirtori, C., Revin, D., Cockburn, J.: Room temperature operation of InAs/AlSb quantum cascade lasers. *Appl. Phys. Lett.* **85**(2), 167–169 (2004)
- Tian, Z., Chen, C., Yang, R.Q., Mishima, T.D., Santos, M.B., Keay, J.C., Johnson, M.B., Klem, J.F.: InAs-based Plasmon-Waveguide Interband Cascade Lasers. *Proceedings of SPIE 7616, Novel In-Plane Semiconductor Lasers IX*, 76161B-9 (2010)
- Vassant, S., Hugonin, J.P., Marquier, F., Greffet, J.J.: Berreman mode and epsilon near zero more. *Opt. Express* **20**(21), 23971–23977 (2012)
- Yang, R.Q.: Infrared laser based on intersubband transitions in quantum wells. *Superlattices Microstruct.* **17**(1), 77–83 (1995)
- Ye, H., Li, L., Hinke, R.T., Yang, R.Q., Mishima, T.D., Keay, J.C., Santos, M.B., Johnson, M.B.: MBE growth optimization of InAs (001) homoepitaxy. *J. Vac. Sci. Technol. B* **31**(001), 03C135 (2013)